

Effect of Small Molecule Modification on Single Cell Pharmacokinetics of PARP Inhibitors:

Greg M. Thurber, Thomas Reiner, Katherine S Yang, Rainer Kohler, Ralph Weissleder

Supplementary Data

Supplementary Materials and Methods

1. Mathematical Model

Plasma

After a bolus intravenous injection, drugs and imaging agents rapidly distribute in the plasma volume before redistribution in peripheral tissues and clearance. A biexponential decay is used to track the concentration over time:

$$\frac{\partial C_{plasma}}{\partial t} = C_{plasma,0} (Ae^{-k_{\alpha}t} + Be^{-k_{\beta}t})$$

where C_{plasma} is the concentration of total drug (protein bound and free drug) in the blood plasma, t is time, $C_{plasma,0}$ is the initial drug concentration, A is the fraction of rapid decay, B is the fraction of slow decay ($A+B = 1$), k_{α} is the redistribution phase rate constant, and k_{β} is the clearance phase rate constant.

Tissue

For drug in the tissue, a two-compartment model is used where both the free drug and non-specifically immobilized drug (e.g. non-specific cell uptake) are lumped in as single compartment and specific target-bound drug forms the second compartment. This assumes rapid equilibrium between non-specifically immobilized drug and free drug.

For free and non-specifically bound drug, the void fraction is set to 1 since the drug is assumed to distribute between the interstitial and intracellular space (which is in contrast to macromolecular simulations (1)). The effective diffusion coefficient is adjusted (2) for a linear immobilized fraction non-specifically bound in cells:

$$D_{eff} = \frac{D}{1 + R} = \frac{D}{1 + \left(\frac{C_{immobile}}{C_{free}}\right)}$$

where D is the diffusion coefficient in the absence of non-specific immobilization, D_{eff} is the diffusion coefficient in tissue with non-specific immobilization, $C_{immobile}$ is the concentration of drug non-specifically bound, and C_{free} is the free drug concentration. Also note that $C_{total} = C_{immobile} + C_{free} = C_{free}(1 + R)$.

The overall drug concentration in the tissue is then:

$$\frac{\partial C_{total}}{\partial t} = D_{eff} \left[\frac{\partial^2 C_{total}}{\partial x^2} + \frac{\partial^2 C_{total}}{\partial y^2} \right] - \frac{k_{bind}}{1 + R} C_{total}(T_0 - B) + k_{release} B$$

$$\frac{\partial B}{\partial t} = \frac{k_{bind}}{1 + R} C_{total}(T_0 - B) - k_{release} B$$

where x and y are the spatial dimensions, k_{bind} is the effective rate of specific binding (in units of inverse free drug concentration and inverse time), T_0 is the total specific target concentration, B is the bound target concentration, and k_{release} is the effective dissociation rate constant in the tissue. These rates are not necessarily equal to the intrinsic binding and dissociation rates to the target protein, since these values were fit to *in vitro* cell culture data that incorporates cellular uptake and transport to the nucleus. It is also assumed that the target concentration is constant over the time scale of the experiment:

$$T_0 = B + T$$

Boundary Conditions

The boundary conditions on the outside edge of the rectangular domain are no-flux (Neumann) conditions:

$$\begin{aligned} \frac{\partial C_{\text{total}}}{\partial x} &= 0 & \frac{\partial C_{\text{total}}}{\partial y} &= 0 \\ \frac{\partial B}{\partial x} &= 0 & \frac{\partial B}{\partial y} &= 0 \end{aligned}$$

The bound drug adjacent to the capillaries is also a Neumann boundary condition:

$$\frac{\partial B}{\partial r} = 0$$

For the capillary boundary condition for total drug (C_{total}), a Robin boundary condition is used, matching the flux across the capillary wall to the diffusive flux in the tissue:

$$\begin{aligned} D_{\text{eff}} \frac{dC_{\text{total}}}{dr} &= P(f_{\text{free}} C_p - C_{\text{free}}) \\ D_{\text{eff}} \frac{dC_{\text{total}}}{dr} + P \frac{C_{\text{total}}}{1 + R} &= P f_{\text{free}} C_p \end{aligned}$$

where r is normal to the capillary surface, P is the capillary permeability, and f_{free} is the fraction of drug not bound to plasma proteins.

Finite Element Model

For the two compartment finite element model, a two-dimensional finite element mesh was drawn using a vascular probe (500 kDa dextran labeled with Pacific Blue (Invitrogen)) to delineate the vessels. A Delaunay triangulation algorithm in Matlab (Mathworks) was used to generate a mesh. The equations listed above were entered into the PDE solver using explicit time steps and reducing the step size until no overshoot occurred in binding between the two coupled compartments. The two-dimensional simulation is valid in this scenario since prior to injection, the tissue volume was scanned to ensure no vessels were immediately above or below the imaging plane. In addition, the high plasma protein binding reduces the drop in plasma concentration along the length of the vessels, so the boundary conditions are approximately equal along all capillary surfaces.

To visualize the nuclear versus perinuclear uptake, a nuclear mask was incorporated in the results. The concentration of specifically bound probe is shown within the nuclear sized repeating circles which represent the nucleus where PARP1 is located(3). The non-specifically immobilized and free drug concentration is shown outside the nucleus. Given the heterogeneous structure of cells within a tumor, a continuum model was used to simulate the drug distribution, and the nuclear mask helps interpret the results.

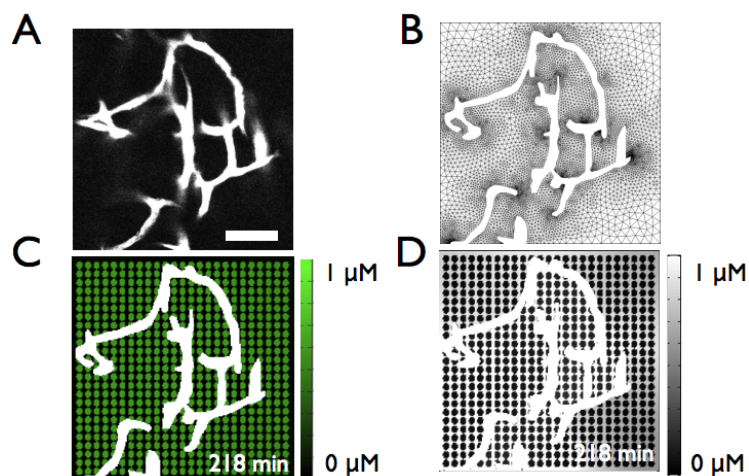


Figure S1. Finite Element Model Approach

A. Macromolecular probe outlining the blood vessels in vivo. B. Finite element mesh over the tissue space between the vessels. C. Olaparib-BodipyFL distribution 3 hrs and 38 min after injection predicting primarily nuclear labeling. D. Olaparib-Bodipy650 distribution is predicted to be perinuclear after 3 hrs and 38 min.

Summary of Parameters

Table S1. Parameter Values for Model

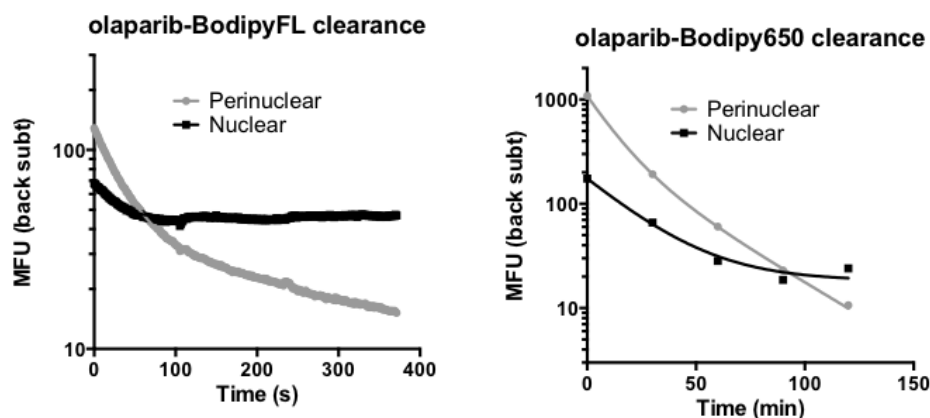
Parameter	Name	olaparib-BodipyFL	olaparib-Bodipy650	Reference
C_0	Initial plasma dose	7.0 μM	22.8 μM	measured
A	Fraction alpha decay	0.77	0.91	measured
$t_{1/2,\alpha}$	Redistribution half-life	5.16 min	7.68 min	measured
$t_{1/2,\beta}$	Clearance half-life	59.4 min	92.5 min	measured
f_{free}	Free fraction in plasma	0.0077	0.0078	measured
P	Permeability	4.7 $\mu\text{m/s}$	0.46 $\mu\text{m/s}$	measured
R	Immobile to free ratio in tissue	18	381	measured
D	Diffusion coefficient	300 $\mu\text{m}^2/\text{s}$	250 $\mu\text{m}^2/\text{s}$	(4)
k_{bind}	Effective binding rate	0.0105/ $\mu\text{M/s}$	0.0014/ $\mu\text{M/s}$	measured
k_{release}	Effective release rate	1.41 $\times 10^{-4}/\text{s}$	1.29 $\times 10^{-4}/\text{s}$	calculated
T_0	Target concentration	3.0 μM	3.0 μM	Measured and (5)

2. Cellular Uptake Kinetics

Cell uptake and wash-out was measure on an inverted microscope at 37°C and 5% CO₂. A time lapse series was initiated prior to the addition of cell culture media with 1 μM of the given probe. Images were taken over the course of 6.2 min (olaparib-BodipyFL) or 46.8 min (olaparib-Bodipy650). Regions of interest were drawn outside the cell, within the perinuclear region, and inside the nucleus identified by a nuclear stain. After subtracting off the background intensity (outside the cell), the values were fit to a mono-exponential function using Prism software. For wash-out experiments, the cells were incubated with 1 μM concentrations for 1 hr, quickly washed in media, and imaged under 37°C and 5% CO₂ in cell culture media. The background signal was subtracted from perinuclear and nuclear signal. Here, the decrease in fluorescence for the perinuclear region was biexponential in nature, possibly due to a build-up of probe within the culture media. A weighted average of the two phases was reported in the table. For the perinuclear to nuclear ratio at a 1 μM added drug concentration, the background contribution was subtracted from each signal. Since the nuclear signal included a contribution from the nuclear envelope (part of the endoplasmic reticulum, ER), the intensity was measured after the initial washout of probe from the ER (representing signal from the nucleus itself). The signal was then adjusted for the larger volume of the cell relative to the nucleus. The ratio represents the amount of total cell drug outside of the nucleus to the total drug inside the nucleus.

Figure S2. Cellular Clearance Data

The clearance of probe around the nucleus dropped in a biexponential pattern, while the nuclear signal had an initial drop over the rapid washout phase from the perinuclear region, likely corresponding to probe in the nuclear envelope, followed by retained signal. At later times the nuclear signal was higher than the perinuclear signal. Note the log scale on the y-axis and different time scales (seconds versus minutes) on the x-axis.



Supplemental References

1. Thurber GM, Schmidt MM, Wittrup KD. Antibody tumor penetration: Transport opposed by systemic and antigen-mediated clearance. *Adv Drug Deliv Rev.* 2008;60(12):1421-34.
2. Crank J. *The Mathematics of Diffusion.* 2 ed. Oxford: Clarendon Press; 1975.
3. Thurber GM, K.S. Yang, T. Reiner, R.H. Kohler, P. Sorger, T. Mitchison, and R. Weissleder. Single-cell and subcellular pharmacokinetic imaging allows insight into drug action in vivo. *Nature Communications.* 2013;4:1504.
4. Pruijn FB, Sturman JR, Liyanage HDS, Hicks KO, Hay MP, Wilson WR. Extravascular transport of drugs in tumor tissue: Effect of lipophilicity on diffusion of tirapazamine analogues in multicellular layer cultures. *J Med Chem.* 2005;48(4):1079-87.
5. D'Amours D, Desnoyers S, D'Silva I, Poirier GG. Poly(ADP-ribosyl)ation reactions in the regulation of nuclear functions. *Biochem J.* 1999;342:249-68.